Compressive Strength of Square Short Concrete Columns reinforced with GFRP Bars produced with Recycled Demolition Aggregate

Omar Taha Mohammed
Department of Civil Engineering, College of Engineering, University of Tikrit, Tikrit, Iraq
Omer.taha@st.tu.edu.iq (corresponding author)

Hasan J. Mohammed
Department of Civil Engineering, College of Engineering, University of Tikrit, Tikrit, Iraq
dr.hasssanjassim@tu.edu.iq

Received: 5 August 2024 | Revised: 25 August 2024 and 3 September 2024 | Accepted: 4 September 2024

 DOI: https://doi.org/10.48084/etasr.8626

ABSTRACT

This study experimentally investigated the compressive strength of short concrete columns reinforced with steel or Glass Fiber Reinforced Polymer (GFRP) bars, using normal aggregate, Recycled Demolition Aggregate (RDA), or Recycled Demolition Concrete (RDC). The study variables included the concrete aggregate type, percentage of aggregate replacement, percentage of cement replaced by Micro Silica Fume (MSF), percentage of added Super-Plasticizer (SP), and the main reinforcement material. Twenty column specimens with dimensions of 150 mm × 150 mm × 700 mm were tested, with ten of them having been reinforced using steel bars and ten using GFRP bars. The results indicated that columns with GFRP bars had higher ultimate load values than their steel-reinforced counterparts. However, the ultimate load of the columns with replaced aggregate was lower than that of the reference column with normal concrete and decreased with an increasing percentage of replaced aggregate. These findings provide insights into the potential use of recycled demolition materials and GFRP reinforcement in short concrete columns while highlighting the impact on compressive strength and ductility.

Keywords-GFRP bars; short concrete columns; recycled demolition aggregate; recycled demolition concrete; micro silica fume; superplasticizer

I. INTRODUCTION

Concrete columns play an important role in the design and construction of several buildings and structures. However, they can be damaged by extreme loads, such as shocks, explosions, earthquakes, changes in structural use and function, corrosion, and chemical reactions [1-3].

Many construction projects in Iraq have reached the end of their design life or have not been built according to the urban development. Some have also been demolished because of the war. The demolition and upkeep of these structures generate a considerable amount of concrete debris. Environmental laws and the rising costs of natural aggregate production have led to the implementation of new guidelines and suggestions in several western countries [4-6]. The low corrosion resistance of steel reinforcement and the requirement to increase the service life of reinforced concrete buildings have driven the use of Glass Fiber Reinforced Polymer (GFRP) bars in structural construction [7].

Authors in [8] conducted research on recycled aggregates made from construction and demolition debris and their application in the construction of concrete. Epoxy resin was applied to the recycled aggregates to reduce water absorption. This study demonstrates that high-quality concrete can be produced using recycled aggregates derived from concrete specimens that have undergone site testing. The split tensile and compressive strengths of the recycled aggregate concrete were comparable to those of the regular concrete. Saturated surface-dry coarse aggregates can be utilized to increase the low slump value of recycled aggregate concrete.

The properties of concrete after replacing coarse aggregate with demolished column waste in various proportions of 10, 20, 30, 40, 50, and 100% were studied in [9]. The results showed that the compressive strength was higher than 30 N/mm^2 when up to 30% of the coarse aggregate was replaced. However, the compressive strength dropped 27.11 N/mm^2, slightly above the desired value of 26.6 N/mm^2, when 50% of the aggregate was replaced. Therefore, regular building activities are better suited for concrete with 50% replaced aggregate.

The study in [10] investigated the characteristics of concrete made from Recycled Demolition Aggregate (RDA).

Through the experimental substitution of RDA for 0%, 25%, 50%, 75%, and 100% of the weight of gravel, five RDA concrete ratios were created. In addition, silica fume was used instead of 10% cement. 0.5%, 1%, and 1.5% of steel fibers were also added. RDA was treated with cement mortar, and an admixture of Super-Plasticizer (SP) was applied to 1% of the total cementitious material. Tests of the concrete density, splitting tensile strength, compressive strength, and modulus of rupture were conducted. According to the test results, RDA concrete has a lower rupture modulus, splitting tensile strength, and compressive strength when its RDA ratio is higher than that of normal concrete. Approximately 9% less density than regular concrete was observed in RDA concrete.

The behavior of columns made of recycled aggregates with axial loads was studied in [11]. The recycled aggregates were obtained from the remnants of earlier concrete projects and utilized instead of natural aggregates. To obtain 28 MPa, several concrete compositions were tested using recycled aggregates ranging from 0 to 50% of the total coarse aggregate. Another variable that was considered was the impact of steel fibers, whose volumes ranged from 0 to 2% of the concrete composition. The experiment demonstrated that the quantity of recycled aggregates in the concrete mixture affects its strength. Recycled aggregates had no influence on the strength of the concrete and enhanced the load-bearing capacity of the column models when they comprised less than 30% of the total aggregates. Additionally, the load-bearing capacity of the concrete columns made with more than 30% recycled aggregate was improved by the steel fibers.

Authors in [12] studied the compressive behavior of reinforced concrete columns produced from recycled materials under monotonic uniaxial loads. Seventeen columns of varying types, qualities, and quantities of recycled coarse and fine aggregates were examined. The results demonstrate that as the amount of recycled coarse aggregate replacement increased, the maximum axial load capacity decreased by roughly 6-8% compared to columns with natural aggregate. However, the recycled fine aggregate had no effect on the axial strength of the column.

Authors in [13] conducted a study on the performance of circular concrete columns that were reinforced with GFRP bars and spirals when subjected to axial load. The test parameters encompassed the reinforcing type, specifically GFRP and steel bars, as well as the longitudinal reinforcement ratio and the spacing of spirals. Most of the tested columns exhibited two peak loads. The test findings indicated that the GFRP Reinforced Concrete (RC) columns displayed a behavior comparable to that of the steel-RC columns. Nevertheless, the GFRP-RC columns exhibited a marginally reduced initial peak load compared with their steel-reinforced counterparts. Incrementing the GFRP reinforcement ratio marginally increased the column capacity. The highly restrained columns demonstrated superior ductile failure and a substantial increase in the second peak load.

Authors in [14] investigated the axial compressive behavior of GFRP columns by building and testing five columns under axial concentric stress. The concrete contained two types of fibers: polyvinyl alcohol (PVA) and polypropylene (PPF). Two forms of transverse confinement (GFRP hoops and GFRP spirals) were offered. The results disclosed that the GFRP columns enclosed by GFRP spirals had superior axial strength and ductility indices.

In [15], the structural behavior of GFRP-reinforced recycled aggregate concrete columns (GRAC columns) and steel-bar reinforced recycled aggregate concrete columns (SRAC columns) under concentric and eccentric loads was investigated. Eighteen samples were produced, nine of which had GFRP reinforcement and the remaining nine contained steel bars. The test results revealed that the GRAC columns had a lower axial strength (up to 7.79%) and greater ductility indices (up to 4%) than the SRAC columns. The failure mechanisms and cracking patterns of the GRAC and SRAC columns were comparable.

The effect of recycled aggregate on the behavior of tied reinforced fibrous rectangular short columns was explored in [16]. The study showed that when adding 50% of normal aggregates along with 50% of recycled aggregates, a decrease of 10%, 18%, 30%, and 22% in the compressive strength, splitting tensile strength, flexural strength, and elasticity module was, respectively, observed. When 100% normal aggregates were replaced with 100% recycled aggregates, a decrease of 30%, 35%, 58%, and 63% was evidenced in the same sequence.

II. RESEARCH SIGNIFICANCE

The main objective of this study was to experimentally investigate the compressive strength of square-based short concrete columns made with demolition aggregate or concrete reinforced with steel or GFRP bars. The parameters that were varied in the preparation of the samples included the concrete aggregate type (normal, RDA, or Recycled Demolition Concrete (RDC)), percentage of aggregate that was replaced, percentage of cement replaced by Micro Silica Fume (MSF), percentage of added SP, and the main reinforcement material.

III. EXPRIMENTAL PROCEDURE AND MATERIAL PROPERTIES

The experimental work involved casting and testing 20 specimens to investigate the compressive strength of short RC columns made from RDA or RDC and reinforced with steel or GFRP rebars. This section also illustrates the testing of the mixes of the ten types of concrete. The experimental work entailed casting 20 RC columns with dimensions of 150 mm × 150 mm and 700 mm in height. Ten specimens were reinforced with steel bars of 8 mm in diameter, while the others were reinforced with GFRP bars of 10 mm in diameter. All specimens were reinforced with steel ties of 6 mm in diameter. Table I presents the details of the tested columns. The column specimens were code named to easily reveal their content. Therefore, the samples were named in the form of X#-Z-#1-#2. X takes the values N, A, and C for the normal, RDA, and RDC aggregate types used, respectively. The accompanying number in X denotes the percentage of normal aggregate which was replaced. Z represents the bar type: St stands for steel and Gf for GFRP bars. The #1 takes the values of 0 or 10 according to the MSF percentage in the mix. Number #2 takes the values 0

or 1 according to the percentage of SP added to the mix. A schematic of the tested short columns is portrayed in Figure 1.

Table II lists the quantities (in Kg/m^3) of the materials required to form the concrete mix design. The RDA and RDC replaced 50% and 100% of the coarse aggregate weight. Additionally, in some mixes, 10% of the cement was replaced by MSF and SP was added at cement weight of 1 %. Figure 2 depicts the wooden molds and reinforcing cages (steel or GFRP). Figure 3 illustrates the test setup and instrumentation utilized.

TABLE I. DETAILS OF THE RC COLUMN SAMPLES

Sample	Aggregate type	Percentage of replaced aggregate (%)	Main bars type	Cement replaced by MSF (%)	SP added (%)
N-St-0-0	Normal	-	Steel	0	0
A50-St-0-0	RDA	50	Steel	0	0
A50-St-0-1	RDA	50	Steel	0	1
A50-St-10-1	RDA	50	Steel	10	1
C50-St-10-1	RDC	50	Steel	10	1
A100-St-0-0	RDA	100	Steel	0	0
C100-St-0-0	RDC	100	Steel	0	0
A100-St-0-1	RDA	100	Steel	0	1
A100-St-10-1	RDA	100	Steel	10	1
C100-St-10-1	RDC	100	Steel	10	1
N-Gf-0-0	Normal	-	GFRP	0	0
A50-Gf-0-0	RDA	50	GFRP	0	0
A50-Gf-0-1	RDA	50	GFRP	0	1
A50- Gf-10-1	RDA	50	GFRP	10	1
C50-Gf-10-1	RDC	50	GFRP	10	1
A100-Gf-0-0	RDA	100	GFRP	0	0
C100-Gf-0-0	RDC	100	GFRP	0	0
A100-Gf-0-1	RDA	100	GFRP	0	1
A100-Gf-10-1	RDA	100	GFRP	10	1
C100-Gf-10-1	RDC	100	GFRP	10	1

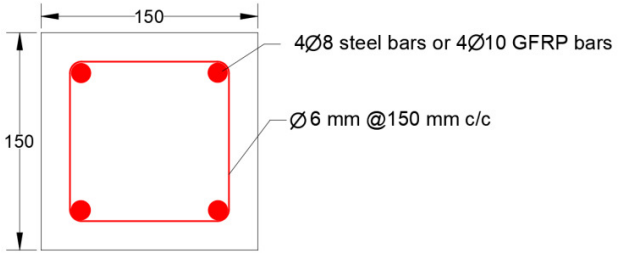

Fig. 1. Details of samples.

TABLE II. CEMENT MIXTURE DESIGN

#	Water	Cement	Sand	MSF	SP	Aggregate			Replaced aggregate (%)
						Normal	RDA	RDC	
1	205	420	652	-	-	990	-	-	0
2	205	420	652	-	-	495	495	-	50
3	200	420	652	-	4.2	495	495	-	50
4	200	378	652	42	4.2	495	495	-	50
5	200	378	652	42	4.2	495	-	495	50
6	205	420	652	-	-	0	990		100
7	205	420	652	-	-	0	-	990	100
8	200	420	652	-	4.2	0	990	-	100
9	200	378	652	42	4.2	0	990	-	100
10	200	378	652	42	4.2	0	-	990	100

All quantities are given in kg/m^3.

Fig. 2. Wood molds and reinforcing cages.

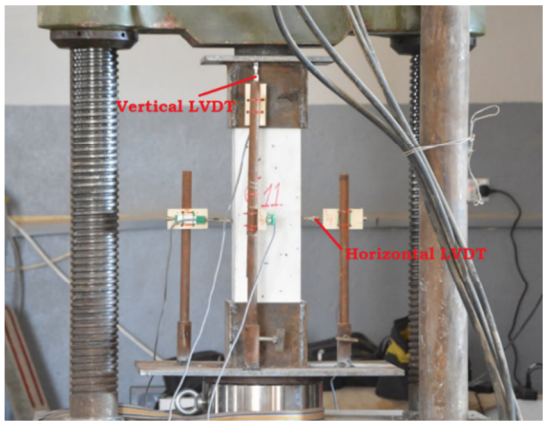

Fig. 3. Test setup and instrumentation.

IV. RESULTS AND DISCUSSION

The results of the hardened concrete used for the mixes are presented in this section. In addition, the results of the 20 short-column specimens, which were tested to study the influence of several parameters on their structural behavior, are presented.

A. Evaluation of Hardened Concrete

Ten concrete mixes were evaluated for their density, compressive strength, modulus of rapture, and splitting tensile strength after 28 days. The results are provided in Table III.

TABLE III. RESULTS OF CONCRETE MIXES

Mix No.	Compressive strength fcu (MPa)	Modulus of rupture fr (MPa)	Splitting tensile strength fct (MPa)	Density (kg/m^3)
1	41.8	3.971	3.553	2445
2	37.6	3.762	3.379	2310
3	39.1	3.839	3.488	2331
4	40.6	3.916	3.499	2322
5	38	3.784	3.39	2294
6	35	3.637	3.245	2288
7	33.7	3.563	3.194	2302
8	35.1	3.641	3.259	2301
9	36.7	3.718	3.325	2300
10	36.1	3.685	3.303	2222

B. Evaluation of Reinforced Concrete Samples

The 20 column specimens were divided into two groups according to the type of main reinforcement bars (ten with steel and ten with GFRP). The results for all columns, including the load-carrying capacity (Pmax), axial displacements measured over the full height of the specimen, and corresponding lateral displacements at the mid-height of the specimen, are listed in Table IV. Figure 4 showcases a comparison of the load-bearing capacities of all specimens.

TABLE IV. EVALUATION THE RC COLUMN SAMPLES

Bars	Sample	Load carrying capacity, Pmax (kN)	At ultimate load	
			Axial displacement (mm)	Mid-height lateral displacement (mm)
Steel	N-St-0-0	771.4	3.7	2.04
	A50-St-0-0	694.26	3.5	1.93
	A50-St-0-1	721.26	3.6	1.98
	A50-St-10-1	749.03	3.7	2.04
	C50-St-10-1	701.2	3.5	1.93
	A100-St-0-0	645.9	3.51	1.94
	C100-St-0-0	621.75	3.4	1.87
	A100-St-0-1	647.98	3.6	1.98
	A100-St-10-1	677.29	3.66	2.02
	C100-St-10-1	666.5	3.64	2.01
GFRP	N-Gf-0-0	842.45	3.56	1.96
	A50-Gf-0-0	760	3.621	1.99
	A50-Gf-0-1	777.5	3.68	2.03
	A50- Gf-10-1	817	3.76	2.07
	C50-Gf-10-1	766.5	3.735	2.05
	A100-Gf-0-0	705.4	3.6	1.983
	C100-Gf-0-0	680	3.59	1.98
	A100-Gf-0-1	706	3.6	1.98
	A100-Gf-10-1	740	3.62	1.99
	C100-Gf-10-1	726	3.61	1.986

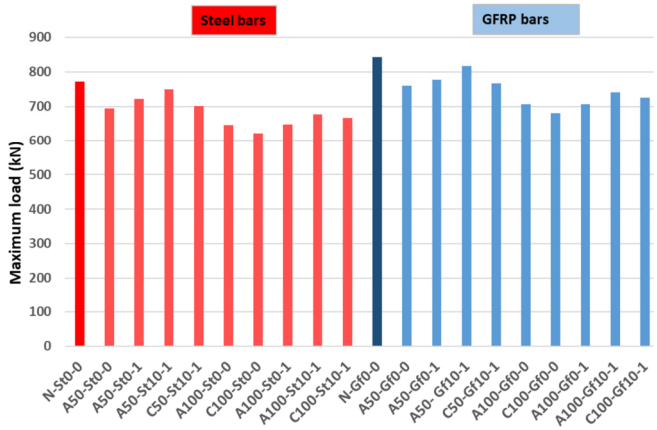

Fig. 4. Comparison of the load-carrying capacities of all column specimens.

C. Load Carrying Capacity of Column Samples.

1) Effect of Bars Type on Pmax

As evidenced in Figure 4 and Table V, the samples with GFRB bars exhibited higher ultimate loads than those with steel bars. This is because the tensile strength of the GFRP bars was higher than that of the steel bars. Table V demonstrates that the maximum load increased when the steel bars were replaced with GFR ranging between 7.79 and 9.47%. A greater increase (9.47%) in the maximum load was noted for the sample A50-Gf-0-0 (50% RDA + 0% MSF + 0% SP). The lowest increase of 7.79% was observed for the sample A50-Gf-0-1 (50% RDA + 0% MSF + 1% SP).

TABLE V. EFFECT OF BARS TYPE ON PMAX

Sample	Pmax (kN)	% increase in Pmax by replacing steel bars with GFRP
N-St-0-0	771.4	Reference
N-Gf-0-0	842.45	9.21
A50-St-0-0	694.26	Reference
A50-Gf-0-0	760	9.47
A50-St-0-1	721.26	Reference
A50-Gf-0-1	777.5	7.79
A50-St-10-1	749.03	Reference
A50- Gf-10-1	817	9.07
C50-St-10-1	701.2	Reference
C50-Gf-10-1	766.5	9.31
A100-St-0-0	645.9	Reference
A100-Gf-0-0	705.4	9.21
C100-St-0-0	621.75	Reference
C100-Gf-0-0	680	9.37
A100-St-0-1	647.98	Reference
A100-Gf-0-1	706	8.95
A100-St-10-1	677.29	Reference
A100-Gf-10-1	740	9.26
C100-St-10-1	666.5	Reference
C100-Gf-10-1	726	8.93

2) Effect of % Replaced Aggregate and the Type on Pmax

Table VI compares the Pmax depending on the aggregate type and amount in the concrete mix. The maximum load decreased in the samples where RDA or RDC was used. Regarding the group of samples with steel bars, Pmax decreased in accordance with the percentage of the replaced aggregate. The highest Pmax of the columns with steel bars and RDA aggregate ranged between 645.9 and 749.03 kN, whereas for the columns with RDC aggregate, the Pmax was between 621.75 and 701.2 kN. Columns with RDA exhibited slightly higher maximum load values than those with RDC. This is because RDA aggregate contains more impurities and air voids, while adhering mortar and air voids also have high water absorption. However, the Pmax of the samples with aggregate replacement was lower than that of the reference samples and reduced up to 19.39% for the sample C100-Gf-0-0 (100% RDC + 0% MSF + 0% SP). The minimum drop of 2.9 in Pmax was observed in the sample A50-St-10-1 (50% RDA + 10% MSF + 1% SP).

Similarly to the group of samples with steel bars, Pmax decreased with the amount of the replaced aggregate in the samples with GFRP bars. The highest maximum load of the columns with GFPR bars and RDA aggregate ranged between 705.4 and 817 kN, whereas for the columns with RDC aggregate, Pmax was between 680 and 766.5 kN. Columns with RDA exhibited slightly higher maximum load values than those with RDC. This is because the RDA aggregate has a higher water absorption capacity and contains more impurities and air gaps. Furthermore, for samples with GFRP bars, the highest decrease in Pmax of 19.3% was observed in the sample

C100-Gf-0-0 (100% RDC + 0% MSF + 0% SP), and a lower value of 3% was noted in the sample A50-Gf-10-1 (50% RDA + 10% MSF + 1% SP).

TABLE VI. EFFECT OF REPLACED AGGREGATE TYPE AND PERCENTAGE OF REPLACEMENT ON PMAX

Sample	Pmax (kN)	% Decrease in Pmax with respect to reference
N-St-0-0	771.4	Reference
A50-St-0-0	694.26	10
A50-St-0-1	721.26	6.5
A50-St-10-1	749.03	2.901
C50-St-10-1	701.2	9.1
A100-St-0-0	645.9	16.3
C100-St-0-0	621.75	19.39
A100-St-0-1	647.98	16
A100-St-10-1	677.29	12.2
C100-St-10-1	666.5	13.6
N-Gf-0-0	842.45	Reference
A50-Gf-0-0	760	9.8
A50-Gf-0-1	777.5	7.7
A50- Gf-10-1	817	3
C50-Gf-10-1	766.5	9
A100-Gf-0-0	705.4	16.3
C100-Gf-0-0	680	19.3
A100-Gf-0-1	706	16.2
A100-Gf-10-1	740	12.2
C100-Gf-10-1	726	13.8

3) *Effect of MSF and SP on Pmax*

SP is utilized to improve the properties of concrete. As shown in Table VII, the addition of SP in the cement mixture had a positive impact and increased the compressive strength of concrete for both the steel- and GFRP-containing samples. The increase in Pmax upon the addition of 1% SP was between 2.3 and 4.2%.

TABLE VII. EFFECT OF SP ON PMAX

Sample	Pmax (kN)	% Increase in Pmax with respect to reference
A50-St0-0	694.26	Ref.
A50-St0-1	721.26	3.9
C100-St0-0	621.75	Ref.
A100-St0-1	647.98	4.2
A50-Gf0-0	760	Ref.
A50-Gf0-1	777.5	2.3
C100-Gf0-0	680	Ref.
A100-Gf0-1	706	3.82

In addition to SP, MSF was implemented in the mixture, and its influence on the RC column samples was studied. According to Table VIII, adding MSF increased the compressive strength and decreased the permeability of the concrete, which resulted in a higher Pmax for both the steel and GFRP samples. The increase in the ultimate load, Pmax, due to the addition of 10% MSF was approximately 3.84 to 5.08%. The observed enhancement in both steel and GFRP reinforced samples indicates that MSF can be effectively used in combination with different types of reinforcement materials.

TABLE VIII. EFFECT OF MSF ON PMAX

Sample	Pmax (kN)	% Increase in Pmax with respect to reference
A50-St0-1	721.26	Reference
A50-St10-1	749.03	3.84
A100-St0-1	647.98	Reference
A100-St10-1	677.29	4.52
A50-Gf0-1	777.5	Reference
A50- Gf10-1	817	5.08
A100-Gf0-1	706	Reference
A100-Gf10-1	740	4.82

D. *Load-Displacement Relationships of Specimens*

1) *Effect of Bars Type*

Figures 5-14 depict the relationship between the axial displacement and the applied axial load for all tested samples, differing only in the bar type. It is evident that the column samples containing GFRP bars were stiffer than the corresponding samples with steel bars. This could be attributed to the higher tensile strength of the GFRP bars.

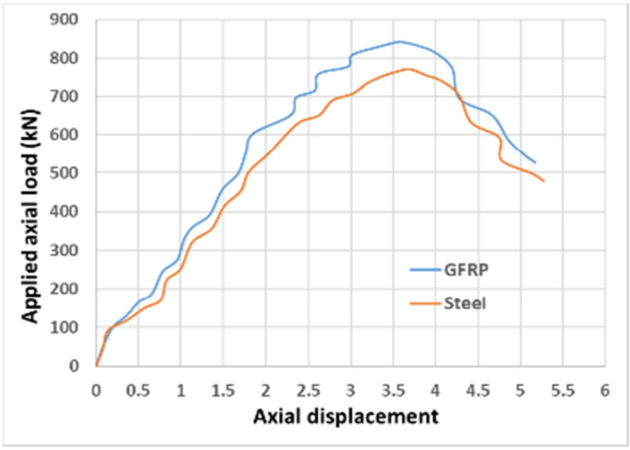

Fig. 5. The applied axial load vs axial displacement for samples N-St-0-0 and N-GF-0-0.

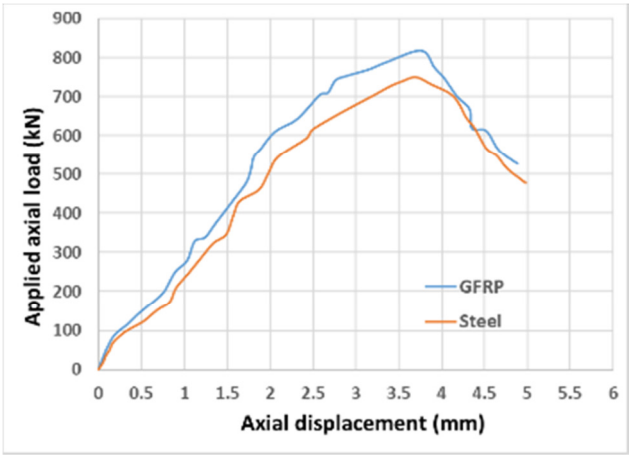

Fig. 6. The applied axial load vs axial displacement for samples A50-St-10-1 and A50-Gf-10-1.

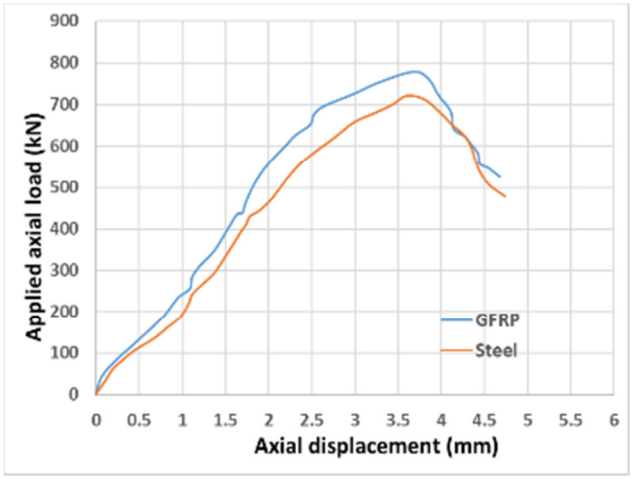

Fig. 7. The applied axial load vs axial displacement for samples A50-St-0-1 and A50-Gf-0-1.

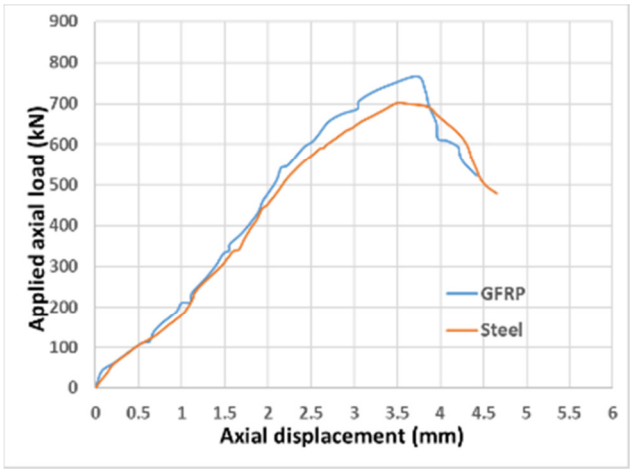

Fig. 8. The applied axial load vs axial displacement for samples C50-St-10-1 and C50-Gf-10-1.

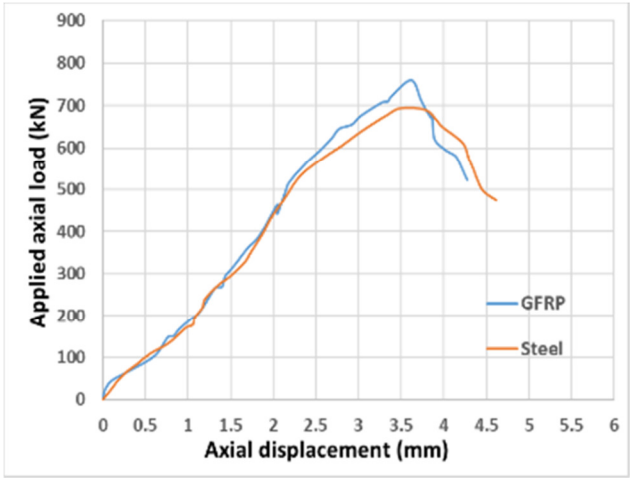

Fig. 9. The applied axial load vs axial displacement for samples A50-St-0-0 and A50-Gf-0-0.

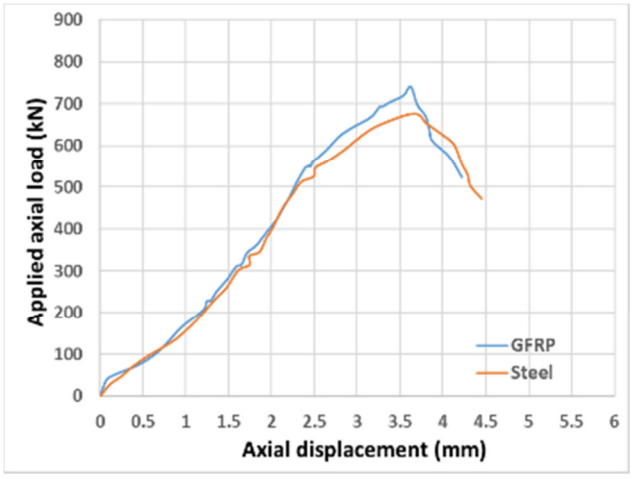

Fig. 10. The applied axial load vs axial displacement for samples A100-St-10-1 and A100-Gf-10-1.

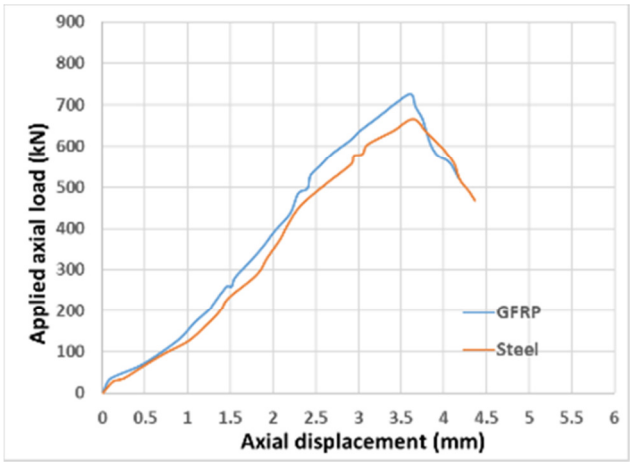

Fig. 11. The applied axial load vs axial displacement for samples C100-St-10-1 and C100-Gf-10-1.

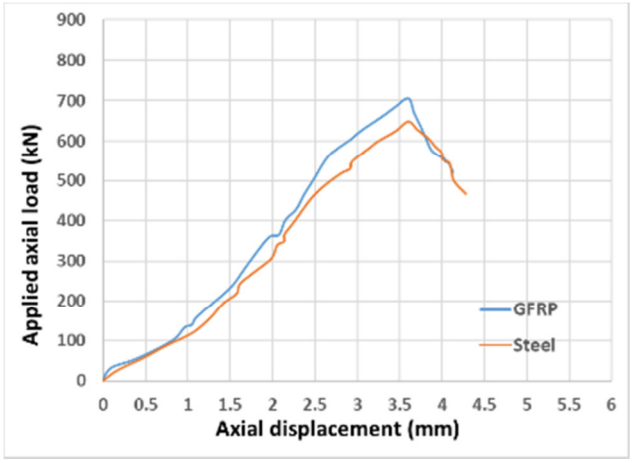

Fig. 12. The applied axial load vs axial displacement for samples A100-St-0-1 and A100-St-0-1.

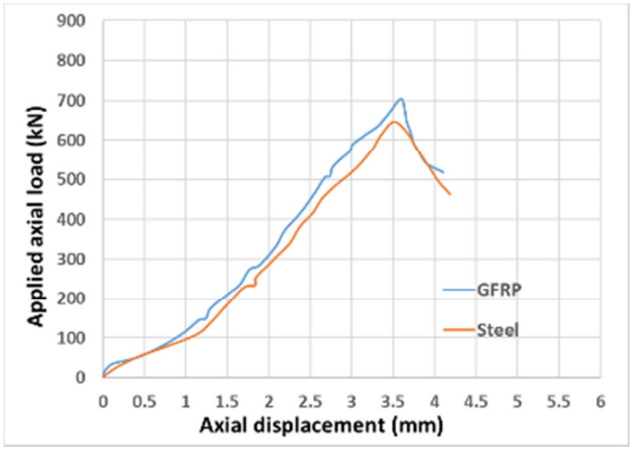

Fig. 13. The applied axial load vs axial displacement for samples A100-St-0-0 and A100-Gf-0-0.

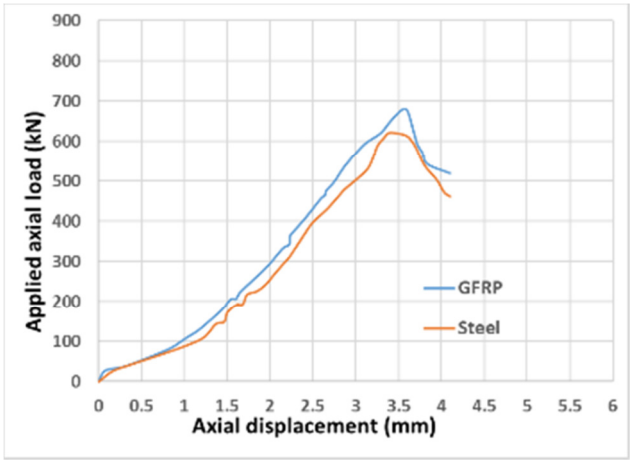

Fig. 14. The applied axial load vs axial displacement for samples C100-St-0-0 and C100-Gf-0-0.

2) *Effect of % Replaced Aggregate and Type*

Figures 15 and 16 portray the effect of the aggregate type and percentage on the relationship between the axial displacement and the applied axial load. Each figure contains four curves for samples with no additives and different types and amounts of aggregates (normal aggregate, 50% RDA, 100% RDA, and 100% RDC). It is clear that replacing the normal aggregate decreased the stiffness of the samples, analogously to the replacement percentage. The samples with RDA exhibited a slightly higher stiffness than those with RDC.

E. Ductility of Column Specimens

The ductility of a structure is defined as its capacity to withstand deformation beyond the point of the first yield deformation while maintaining the ability to support the load. The ductility of the tested samples was estimated deploying an established technique using the displacement ductility ratio as an indicator [17]. The displacement ductility is defined as the ratio between the displacement at the peak load (Δu) and the notional yield displacement (Δy), as illustrated in Figure 17 [17].

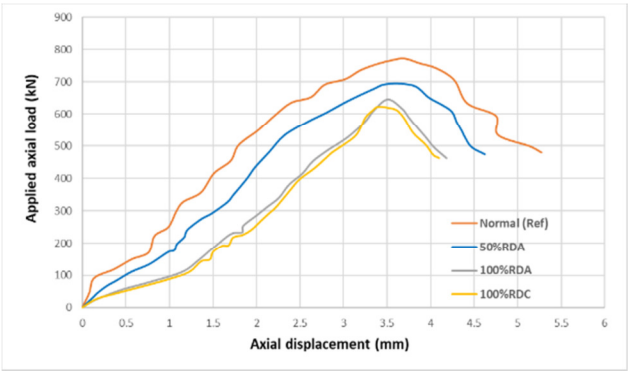

Fig. 15. Comparison of the axial displacement depending on the aggregate type of samples with steel bars and without MSF and SP (N-St-0-0, A50-St-0-0, A100-St-0-0, and C100-St-0-0).

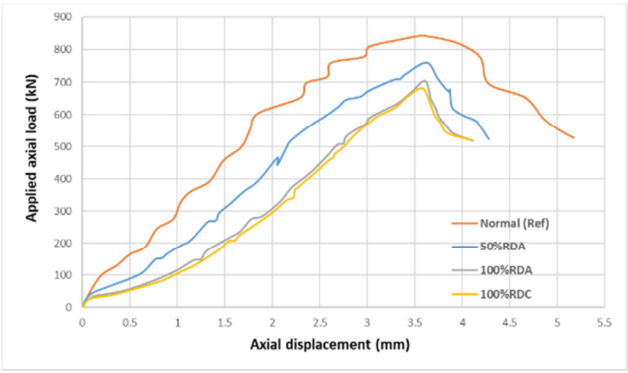

Fig. 16. Comparison of the axial displacement depending on the aggregate type of samples with GFRP bars and without MSF and SP (N-Gf-0-0, A50-Gf-0-0, A100-Gf-0-0, and C100-Gf-0-0).

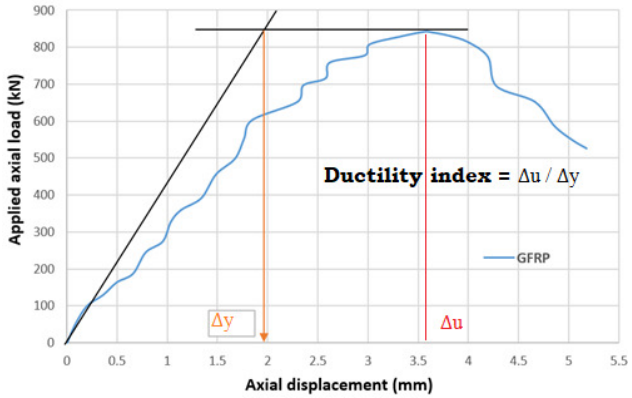

Fig. 17. Procedure to obtain Δy for ductility index for N-Gf-0-0 sample.

Figure 18 manifests a comparison of the ductility index values of the tested columns. The ductility index of the samples decreased with an increasing percentage of the replaced aggregates. Moreover, the ductility index of the samples with steel bars was higher than that of the samples with GFRP bars, because GFRP bars are brittle and prone to cracking or breaking under a sudden load.

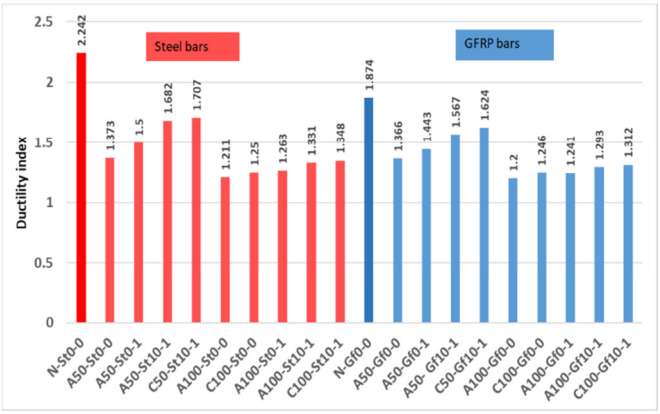

Fig. 18. Comparison of ductility index values for the tested columns.

F. Energy Absorption Capacity of Column Samples

The absorbed energy of the concrete column is defined as the area enclosed by the load-displacement curve until the maximum load is reached, which represents the energy absorption of the concrete column that can be sustained before displaying a significant drop in the load-carrying capacity [18]. The energy absorption capacity of GFRP and steel columns was calculated, and the values obtained are tabulated in Table IX. The absorbed energy of the columns decreased slightly with an increase in the percentage of the replaced aggregate because of the reduction in stiffness. The absorbed energy of the columns of GFRP bars was larger than that of the columns of steel bars.

TABLE IX. ABSORBED ENERGY OF COLUMN SAMPLES

Column designation	Ultimate load Pu (kN)	Energy absorption capacity (kN.mm)
N-St-0-0	771.4	1711.4
A50-St-0-0	694.26	1283
A50-St-0-1	721.26	1430.3
A50-St-10-1	749.03	1599.2
C50-St-10-1	701.2	1317.8
A100-St-0-0	645.9	942.3
C100-St-0-0	621.75	829.3
A100-St-0-1	647.98	1086.8
A100-St-10-1	677.29	1313.5
C100-St-10-1	666.5	1179.8
N-Gf-0-0	842.45	1799
A50-Gf-0-0	760	1426.4
A50-Gf-0-1	777.5	1694.5
A50- Gf-10-1	817	1854.8
C50-Gf-10-1	766.5	1587.6
A100-Gf-0-0	705.4	1107
C100-Gf-0-0	680	1052.7
A100-Gf-0-1	706	1212.4
A100-Gf-10-1	740	1355
C100-Gf-10-1	726	1287.8

G. The Failure Pattern of Columns Samples

Throughout the testing phase, the failure mechanism seen in all steel columns exhibited a steady progression initiated by the separation of a substantial piece of concrete. Subsequently, the appearance of the steel reinforcement became evident, leading to the eventual occurrence of localized failure. In the case of steel columns, the occurrence of cover spalling and buckling of longitudinal reinforcement may be seen, as displayed in Figure 19. Throughout the testing period, the failure mechanism in all the GFRP columns followed a consistent pattern, commencing with the separation of a significant piece of concrete. Subsequently, the presence of GFRP bars became obvious, resulting in localized failure. Figure 20 exhibits the cover spalling and minimum buckling of the longitudinal reinforcement in GFRP columns.

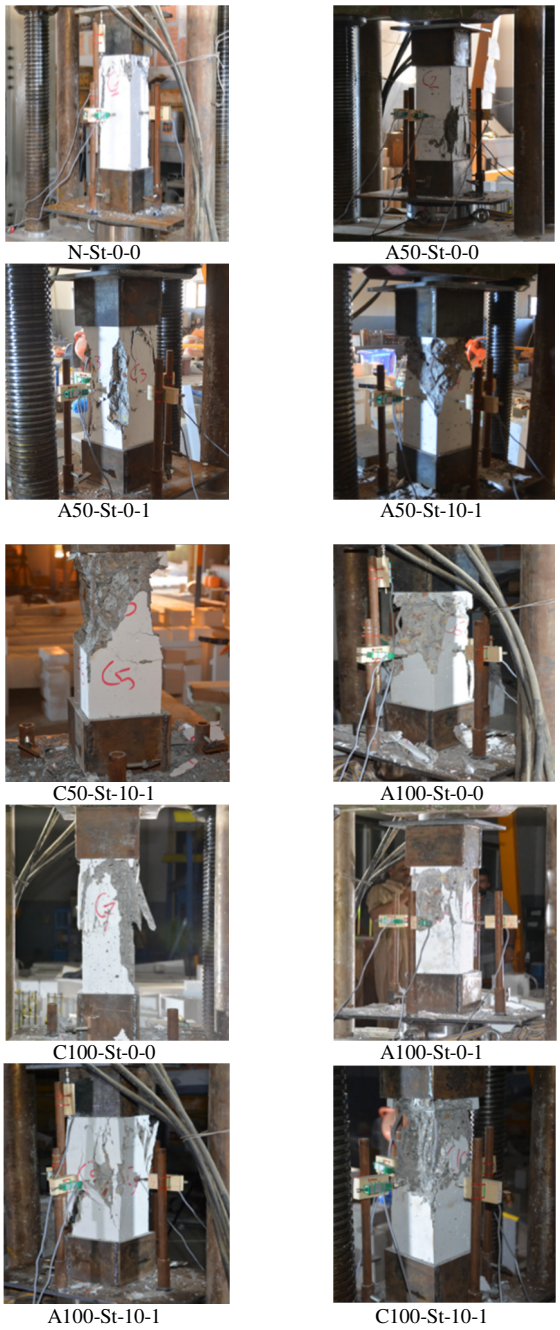

Fig. 19. Failure modes of columns containing steel bars.

Fig. 20. Failure modes of columns containing GFRP bars.

V. CONCLUSIONS

This study experimentally investigated the compressive strength of short concrete columns reinforced with steel or Glass Fiber Reinforced Polymer (GFRP) bars, using normal aggregate, Recycled Demolition Aggregate (RDA), or Recycled Demolition Concrete (RDC). The research variables consisted of the type of concrete aggregate, percentage of each concrete aggregate type, percentage of added Micro Silica Fume (MSF) utilized as a substitute for concrete, percentage of added superplasticizer (SP), and main material employed for reinforcement.

The analysis of the results showed that columns with GFRP bars exhibited 7.79-9.47% higher ultimate load capacities than those of steel-reinforced columns, owing to the higher tensile strength of the GFRP bars. The GFRP-reinforced sample columns demonstrated higher stiffness than that of the steel-reinforced columns throughout loading. This is because the tensile strength of the GFRP bars was higher than that of the steel bars. Increasing the percentage of SP or MSF improved column stiffness.

For steel-reinforced columns, replacing 50% and 100% of the normal aggregate with RDA resulted in 10% and 16.3% decrease in the ultimate load, respectively. For the GFRP-reinforced columns, the drop in the ultimate load was 9.8% and 16.3. When 100% of normal aggregate was replaced with RDC, the ultimate load decreased by 19.39% for the steel-reinforced concrete samples and 19.3% for the GFPR-reinforced concrete samples. Columns with RDA exhibited slightly higher maximum load values than those with RDC. This is because the RDA aggregate contains more impurities and air voids, while adhering mortar and air voids also have high water absorption.

Implementing MSF and SP in the mixture of the concrete had a positive impact on the compressive strength of concrete for both the steel- and GFRP-containing samples. The increase in Pmax upon the addition of 1% SP was between 2.3 to 4.2%. The increase in the ultimate load, Pmax, due to the addition of 10% MSF was approximately 3.84 to 5.08%.

The ductility index decreased slightly with an increasing recycled aggregate content for both the steel and the GFRP columns. The steel-reinforced columns displayed higher ductility than that of the GFRP-reinforced columns. The ductility index of the steel bar columns was larger than that of the GFRP bar columns, since the GFRP bars are brittle and prone to cracking or breaking under sudden loads.

The failure mechanisms were similar for all columns, starting with concrete cover separation and followed by reinforcement exposure and localized failure. Steel columns demonstrated more pronounced cover spalling and longitudinal bar buckling than GFRP columns.

In conclusion, although recycled aggregates reduced the column strength and ductility to some degree, the use of GFRP reinforcement, SP, and MSF helped mitigate these effects. The results provide insights for potentially utilizing recycled demolition materials and GFRP reinforcement in concrete, though further research is needed to optimize mix designs and reinforcement configurations for structural applications.

REFERENCES

[1] C. Zeng, P. Cui, Z. Su, Y. Lei, and R. Chen, "Failure modes of reinforced concrete columns of buildings under debris flow impact," *Landslides*, vol. 12, no. 3, pp. 561–571, Jun. 2015, https://doi.org/10.1007/s10346-014-0490-0.

[2] M. Oad, A. H. Buller, B. A. Memon, N. A. Memon, and S. Sohu, "Flexural Stress-Strain Behavior of RC Beams made with Partial Replacement of Coarse Aggregates with Coarse Aggregates from Old Concrete: Part-2: Rich Mix," *Engineering, Technology & Applied*

Science Research, vol. 8, no. 5, pp. 3338–3343, Oct. 2018, https://doi.org/10.48084/etasr.2129.

[3] M. Oad, A. H. Buller, B. A. Memon, and N. A. Memon, "Impact of Long-Term Loading on Reinforced Concrete Beams Made with Partial Replacement of Coarse Aggregates with Recycled Aggregates from Old Concrete," *Engineering, Technology & Applied Science Research*, vol. 9, no. 1, pp. 3818–3821, Feb. 2019, https://doi.org/10.48084/etasr.2498.

[4] A. Abd Elhakam, A. E. Mohamed, and E. Awad, "Influence of self-healing, mixing method and adding silica fume on mechanical properties of recycled aggregates concrete," *Construction and Building Materials*, vol. 35, pp. 421–427, Oct. 2012, https://doi.org/10.1016/j.conbuildmat.2012.04.013.

[5] H. Rashid and H. Mohammed, "Flexural Behaviour of Recycled Demolition Waste Reinforced Concrete Beams," presented at the Proceedings of 2nd International Multi-Disciplinary Conference - Integrated Sciences and Technologies, Sakarya, Turkey, Turkey, 7-9 September 2021, https://doi.org/10.4108/eai.7-9-2021.2314922.

[6] L. Zeng, L. Li, Z. Su, and F. Liu, "Compressive test of GFRP-recycled aggregate concrete-steel tubular long columns," *Construction and Building Materials*, vol. 176, pp. 295–312, Jul. 2018, https://doi.org/10.1016/j.conbuildmat.2018.05.068.

[7] S. P. Tastani and S. J. Pantazopoulou, "Bond of GFRP Bars in Concrete: Experimental Study and Analytical Interpretation," *Journal of Composites for Construction*, vol. 10, no. 5, pp. 381–391, Oct. 2006, https://doi.org/10.1061/(ASCE)1090-0268(2006)10:5(381).

[8] S. Shahidan, M. A. M. Azmi, K. Kupusamy, S. S. M. Zuki, and N. Ali, "Utilizing Construction and Demolition (C&D) Waste as Recycled Aggregates (RA) in Concrete," *Procedia Engineering*, vol. 174, pp. 1028–1035, Jan. 2017, https://doi.org/10.1016/j.proeng.2017.01.255.

[9] R. Hegde, S. R. K, P. V. Vijaykumar, S. H, A. H. Jakathi, and S. H. Madar, "A Study on Strength Characteristics of Concrete by Replacing Coarse Aggregate by Demolished Column Waste," *International Journal of Engineering Research & Technology*, vol. 7, no. 6, pp. 386–395, Jun. 2018, https://doi.org/10.17577/IJERTV7IS060213.

[10] H. J. Mohammed and Z. S. Sabir, "Properties of Concrete Containing Recycled Demolition Aggregate," *IOP Conference Series: Earth and Environmental Science*, vol. 877, no. 1, Nov. 2021, Art. no. 012029, https://doi.org/10.1088/1755-1315/877/1/012029.

[11] O. S. Farhan, "Effect of Use Recycled Coarse Aggregate on the Behavior of Axially Loaded Reinforced Concrete Columns," *Journal of Engineering*, vol. 25, no. 10, pp. 88–107, Sep. 2019, https://doi.org/10.31026/j.eng.2019.10.07.

[12] W.-C. Choi and H.-D. Yun, "Compressive behavior of reinforced concrete columns with recycled aggregate under uniaxial loading," *Engineering Structures*, vol. 41, pp. 285–293, Aug. 2012, https://doi.org/10.1016/j.engstruct.2012.03.037.

[13] S. El-Gamal and O. AlShareedah, "Behavior of axially loaded low strength concrete columns reinforced with GFRP bars and spirals," *Engineering Structures*, vol. 216, Aug. 2020, Art. no. 110732, https://doi.org/10.1016/j.engstruct.2020.110732.

[14] U. Rafique, A. Ali, and A. Raza, "Structural behavior of GFRP reinforced recycled aggregate concrete columns with polyvinyl alcohol and polypropylene fibers," *Advances in Structural Engineering*, vol. 24, no. 13, pp. 3043–3056, Oct. 2021, https://doi.org/10.1177/13694332211017997.

[15] A. Raza and U. Rafique, "Efficiency of GFRP bars and hoops in recycled aggregate concrete columns: Experimental and numerical study," *Composite Structures*, vol. 255, Jan. 2021, Art. no. 112986, https://doi.org/10.1016/j.compstruct.2020.112986.

[16] J. K. Sahan and E. K. Sayhood, "Effect of recycled aggregate on behaviour of tied reinforced fibrous rectangular short columns," *IOP Conference Series: Earth and Environmental Science*, vol. 779, no. 1, Jun. 2021, Art. no. 012006, https://doi.org/10.1088/1755-1315/779/1/012006.

[17] A. Azizinamini, D. Darwin, R. Eligehausen, R. Pavel, and S. K. Ghosh, "Proposed Modifications to ACI 318-95 Tension Development and Lap Splice for High-Strength Concrete," *ACI Structural Journal*, vol. 96, no. 6, pp. 922–926.

[18] M. S. Abdulraheem, "Effect of Fire Exposed on the Behavior of Reactive Powder Concrete Columns under Concentric Compression Loading," M.S thesis, Department of Civil Engineering, University of Babylon, Iran, 2017.